ELSEVIER

Biophysical Chemistry 60 (1996) 63–77

Biophysical Chemistry

The fluorescence and circular dichroism of proteins in reverse micelles: application to the photophysics of human serum albumin and N-acetyl-L-tryptophanamide

Daniel M. Davis [a], David McLoskey [a], David J.S. Birch [a,*], Paul R. Gellert [b], Rodney S. Kittlety [b], Ronald M. Swart [c]

[a] *Department of Physics and Applied Physics, Strathclyde University, John Anderson Building, 107 Rottenrow, Glasgow G4 ONG, UK*
[b] *Zeneca Pharmaceuticals, Mereside, Alderley Park, Macclesfield, Cheshire SK10 4TG, UK*
[c] *Zeneca Specialities, P.O. Box 42, Hexagon House, Manchester M9 3DA, UK*

Received 11 July 1995; revised 4 January 1996; accepted 29 January 1996

Abstract

Evidence is presented that a compartmentalised protein exists in its native state only within a particular size of aqueous cavity. This behaviour is shown to exist in AOT reverse micelles using fluorescence quenching and circular dichroism (CD) studies of human serum albumin (HSA). In particular, far ultraviolet CD measurements show that a reduction in quencher accessibility to the fluorophore is consistent with the protein being nearest to its native conformation at a waterpool size of around 80 Å diameter. We also show that the biexponential fluorescence decay of N-acetyl-L-tryptophanamide (NATA) in AOT reverse micelles arises from the probe being located in two distinct sites within the interfacial region. The more viscous of these two sites is located on the waterpool side of the interface and the other is located on the oil side of the interface.

Keywords: Human serum albumin (HSA); N-acetyl-L-tryptophanamide (NATA); Fluorescence quenching; Circular dichroism; Reverse micelles; Aerosol OT (AOT)

1. Introduction

Reverse micelles are spontaneously formed colloidal systems with surfactant molecules separating a waterpool from a bulk organic phase. In general, the radius of the encapsulated waterpool is approximately proportional to the molar ratio of water to surfactant denoted as ω_0. The structure of the reverse micelle usually presented is a tightly bound layer of 'frozen' water molecules associated with the surfactant head groups with any excess water forming the 'bulk' waterpool. However, the exact nature of the aqueous phase of reverse micelles is probably more complex and has received much attention [1]. Furthermore, the system is in dynamic equilibrium, but no re-distribution of the reactants occurs on the nanosecond timescale of fluorescence [1]. AOT/iso-octane/water reverse micelles have been widely studied by a variety of techniques and are stable over a relatively large range of waterpool sizes: from no water present to a waterpool diameter

* Corresponding author. Tel.: -44-141-552-4400 ext. 3377; fax: -44-141-552-2891.

PII S0301-4622(96)00016-6

of approximately 130 Å. It should also be noted that there is some ambiguity in the literature over precise use of the terms 'reverse micelles' and 'microemulsions', the latter technically implying larger waterpool sizes. Here the term 'reverse micelles' is used throughout, keeping in line with other relevant papers.

Extraction of proteins from organic solvents by reverse micelles has been widely reported (e.g., [2]), and provides a means for extractive separation and purification of proteins smaller than 100 kDa. Also, it has been suggested that reverse micelles can improve the refolding yield of proteins recovered from bacterial inclusion bodies by isolating the denatured proteins and thus reducing the intermolecular interactions that lead to protein aggregation [3,4]. Aggregation of nascent proteins in vivo is prevented with the help of molecular chaperones such as GroEL. The molecular mechanism for this process involves the incorporation of the protein or protein domains into the cylindrical cavity of the chaperone [5,6] and hence the study of the effects of such a compartmentalisation of proteins is important. Additionally, compartmentalisation of proteins in reverse micelles also allows studies to be made on the effects of hydration on protein dynamics [7,8], and could provide information on the role of hydration in enzyme catalysis, since the total amount of water available to the system can be easily controlled.

Many biological phenomena occur at interfaces, rather than in homogeneous solution, and surface/protein interactions play a key role in the reactions involving membrane proteins. In particular, it has been shown that the lack of water available to the embedded parts of integral membrane proteins encourage the polypeptide chains to form an α-helix when transversing the membrane, in order to maximise the hydrogen bonding between peptide bonds [9]. The very large interfacial region provided by a reverse micellar system can be expected to enhance such effects, as the amphipatic essence of a biological membrane is preserved. Furthermore, a bell-shaped dependence of enzyme activity with waterpool size has been observed for many different proteins in reverse micelles, as reviewed by Khmelnitsky et al. [10]. The waterpool size at which the peak enzyme activity occurs seems to be linearly proportional to the size of the protein used. In fact, the peak activity of many enzymes in reverse micelles is greater than that found in aqueous solution and are said to become 'superactive' [10]. The origin of this enzyme 'superactivity' is not obvious, and its understanding may provide new insights into interfacial phenomena in general.

Despite the widespread use of tryptophan's intrinsic fluorescence as a probe of microenvironment (e.g., [11]), only a small fraction of the work has reported on the photophysics of proteins in reverse micelles (e.g., [7,8,12–19]). The work reported here investigates the interaction between proteins and reverse micelles using various steady-state and time-resolved fluorescence techniques at a range of waterpool sizes in greater detail than previous work. These include measurements of the fluorophore's rotational freedom using anisotropy analysis and the use of the quenching agents carbon tetrachloride and acrylamide or sodium iodide, soluble in non-polar and polar environments respectively, as shown in Fig. 1. Measurements of the far UV circular dichroic characteristics of HSA in the reverse micellar system clarify the molecular interpretations of the trends discovered in fluorescence measurements.

Human serum albumin (HSA) is a widely studied single tryptophan protein whose structure is now known down to the atomic level [20]. The tryptophan residue is located at position 214 amongst a total of 585 amino acids, in a hydrophobic pocket of subdomain IIA important for ligand binding. At neutral pH, the protein is in the N-state, and is 67% helical, with the rest in turns or extended polypeptide chains. From circular dichroism measurements, Desfosses et al. [21] showed that upon incorporation into AOT reverse micelles of $\omega_0 = 22.4$, the helical content of HSA decreases by 15%. Advancing such previous circular dichroism (CD) measurements of proteins in reverse micelles, we report a distinct variation in the protein's conformation with the composition of the reverse micellar solution.

The location of proteins within reverse micellar systems is not obvious, and is important for determining the molecular interactions responsible for the photophysical trends reported here. Pileni [22] suggests 6 models of protein occupancy within a reverse micellar solution, summarised below:

(a) the protein lies in the outer bulk phase (iso-octane)

(b) the protein lies in the external interface (i.e. lies in the iso-octane but in contact with the AOT interface)
(c) the protein is positioned in the waterpool
(d) the protein lies in the internal interface (i.e. lies in the waterpool but is in contact with the AOT interface)
(e) the protein straddles the interface acting as a surfactant
(f) the protein is associated with its own surfactant molecules around it causing a second micellar population.

Throughout this paper we will demonstrate how photophysical techniques can distinguish the above models and show how our results point to the new concept of the compartmentalised protein existing in its native state only at a particular waterpool size. Moreover, in a parallel study, we show that the model compound NATA exists in AOT reverse micelles in two distinct sites on predominantly 'opposite sides' of the oil–water interface. This bimodal distribution of locations is shown to account for the photophysics of NATA in terms of its fluorescence lifetime, quenching and spectral properties in reverse micelles.

2. Materials and methods

L-tryptophan, NATA and HSA were used as received from Sigma. Dioctyl sodium sulfosuccinate (Aerosol OT or AOT) and HPLC grade iso-octane were used as received from Aldrich and Romil, respectively, and a stock solution of 0.25 M AOT/iso-octane was prepared. For solutions of $\omega_0 = 0$ the tryptophan derivative was then added directly, otherwise the relevant derivative was then added to either Trizma buffer (pH 7.1) or purified water. Reverse micelle solutions were then prepared by direct injection of the aqueous solution into the surfactant/hydrocarbon mixture using a microsyringe. If required, the mixture was agitated using a vortex stirrer until clear. Generally, reverse micelles were initially formed at low waterpool sizes and then swollen with subsequent aliquots of pure water or buffer. Concentrations of tryptophan derivative were used such that multiple occupancy would be statistically unlikely with at least 5 reverse micelles per tryptophan-containing molecule. Petit et al. [23] showed that, at least for small proteins such as cytochrome *c*, a Poisson distribution is appropriate for describing the occupancy of the reverse micelles. All experiments were performed at room temperature.

Unlike HSA, NATA dissolved in the reverse micellar solution even when added as a crystalline solid in the absence of any additional water. This is probably due to the relatively small dimensions of the molecule and its amphipatic nature. However, it is also likely that water molecules contained within the crystalline solid help in the solvation of NATA within the AOT/iso-octane system. This is consis-

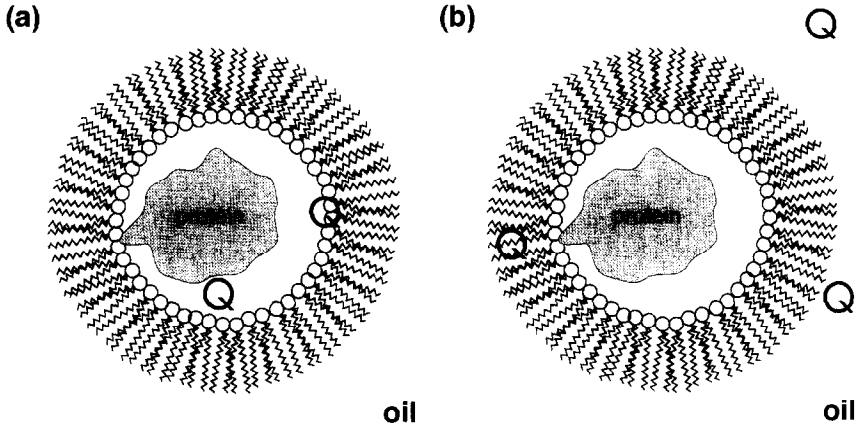

Fig. 1. Schematic diagram of a protein incorporated in a reverse micelle in the presence of quencher molecules in (a) the polar phases, and (b) the non-polar phases.

tent with the formation of a separate phase below the AOT/iso-octane mixture upon the addition of NATA as a crystalline solid before the sample is shaken. However, despite the likelihood of some water being present within a reverse micellar sample prepared with crystalline NATA, this composition is denoted here by $\omega_0 = 0$. Likewise, the amount of water within crystalline HSA is not included in the determination of the ω_0 value. These procedures are consistent with that of previous work (e.g. [7,8]). Also, it is important to note that, for quenching studies of the tryptophanyl derivatives in reverse micelles, the quencher concentrations are calculated with respect to the phase in which they are restricted. That is, the acrylamide concentration is quoted with respect to the solution's water content while the concentration of carbon tetrachloride is quoted with respect to the oil volume used.

Time-resolved fluorescence measurements were made using the technique of single-photon timing. The excitation source was a hydrogen filled coaxial nanosecond flashlamp [24] with wavelength selection obtained using a Kratos GM-200 double monochromator blazed at 240 nm and with a 20 nm bandpass. Unless stated otherwise, excitation was centred at 295 nm. Except for the multi-wavelength single-photon timing array measurement described in 3.1.1, fluorescence emission was selected by either a Schott cut-off filter or a second monochromator, as appropriate, and detected using a Phillips XP2020Q photomultiplier tube. Anisotropy measurements were obtained using Glan–Thompson polarisers with emission at each polarisation being detected alternately at 1-min intervals by automated rotation of the polariser. All data analyses were performed with reconvolution using the IBH software library. The goodness of fit is represented by the normalised χ^2 and errors quoted are three standard deviations as found by the software.

Steady-state quenching results were plotted as the ratio of intensity, I, to the unquenched intensity, I_0, with the molar quencher concentration, $[Q]$. A straight line can be fitted using the familiar Stern–Volmer quenching equation [25]:

$$\frac{I_0}{I} = 1 + K_{SV}[Q] \qquad (1)$$

where K_{SV} is the Stern–Volmer constant. Time-resolved quenching data were plotted and fitted to the familiar time-resolved Stern–Volmer equation [25]:

$$\frac{\tau_0}{\tau} = 1 + K_{SV}[Q] \qquad (2)$$

where τ and τ_0 are the quenched and unquenched lifetimes respectively. The Stern–Volmer quenching constant is related to the quenching rate constant, k_q, as [25]:

$$K_{SV} = k_q \tau_0 \qquad (3)$$

It is well known that Stern–Volmer analysis of quenching is not a complete description of quenching in reverse micellar media because there is a Poissonian distribution of quencher and fluorophore in the individual reverse micelles. Models for quenching in micellar media in several different cases are described, for example, by de Schryver and co-workers [26,27]. However, analysis according to these models is unlikely to be generally practicable such that they are too complex for the resolution of the data reported in this paper. In any case the trends in the quenching data which we report represent a first step, which, as we will demonstrate, are consistent with other findings.

Circular dichroism measurements were performed using a Jobin–Yvon Dichrograph CD6. Subtraction of the background circular dichroism was carried out in each case using unfilled reverse micelles of appropriate composition. To reduce the overall UV absorption, a concentration of 0.05 M AOT in iso-octane and 0.25 mg/ml protein (based on overall volume) was used for the circular dichroism measurements.

3. Results and discussion

3.1. NATA in reverse micelles

N-acetyl-L-tryptophan-amide (NATA) is considered the standard reference compound for tryptophan in proteins by its mimicking of the amino acid's attachment in the backbone chain. Unlike the free amino acid, fluorescence of aqueous NATA is widely recognised to decay monoexponentially [28,29], although recently Gallay et al. [13] have reported a second short decay component at the red edge of the emission. This short lifetime may imply the presence

of a small fraction of NATA in a conformation that is distinct from that producing the longer fluorescence decay component. However, for this work, a 1.35×10^{-4} M solution of NATA in Trizma buffer (pH 7.1) excited at 295 nm and using a 320 nm cut-off filter, was found to decay monoexponentially with a decay time of 2.8 ns, with an associated χ^2 of 1.03. In contrast, the fluorescence decay of NATA in AOT/iso-octane/buffer reverse micelles was found to be more complex.

The fluorescence decay of NATA in AOT/iso-octane/buffer reverse micelles fitted well to a biexponential model (i.e. $0.9 < \chi^2 < 1.2$) throughout all waterpool sizes used ($0 < \omega_0 < 50$). This implies that two different NATA excited states exist within the micellar structure. However, although the complex fluorescence decay of NATA in AOT reverse micelles has been previously observed by Ferreira and Gratton [7] and Gallay et al. [13], the origin of the two distinct excited states of the fluorophore was not ascertained in this earlier work.

In determining the origin of the biexponential decay of NATA in AOT reverse micelles, the location of the fluorophore within the microheterogeneous solution is crucial (see Section 1 for a discussion on the possible sites of probes in reverse micelles). Then it must be determined if the two distinct excited states of NATA arise from the fluorophore occupying two distinct locations within the reverse micellar system (as first suggested in this laboratory [30]) or from two distinct conformations of NATA occupying a single site. There is little debate on this matter in the previous fluorescence studies of NATA in AOT reverse micelles cited above.

The variation in the lifetime components of the NATA fluorescence decay with increasing waterpool size is shown in Fig. 2. Even at high waterpool sizes, i.e. $\omega_0 = 50$, the fluorescence decay is still biexponential indicating that the NATA molecule cannot be positioned completely in the waterpool but is still affected by the micellar interface. Also, as NATA does not dissolve in iso-octane it could not be completely located in the bulk hydrocarbon phase. Therefore, NATA must lie in the interfacial region of the reverse micellar system. This is consistent with the charge distribution on the NATA molecule; the indole group is hydrophobic while the opposite end is

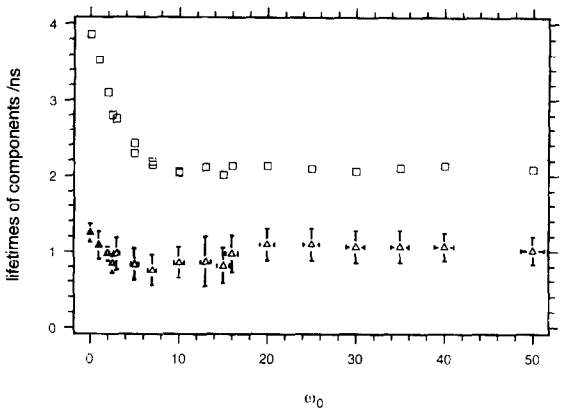

Fig. 2. The change in the two fluorescence exponential decay components of NATA with varying waterpool size in reverse micelles. Waterpool size is represented as the notional value of the molar ratio of water to surfactant, ω_0.

more polar. At $\omega_0 \approx 55$ the NATA-containing reverse micellar structure becomes unstable.

Furthermore, if the NATA molecule is located in two distinct sites then it is likely that the site of NATA giving rise to the long lifetime decay component would be a more polar site as this lifetime component is closer to that of NATA in aqueous solution for which τ ca. 2.8 ns. That is, if it is located in two distinct sites, then it is the excited state of NATA giving rise to the long lifetime component that is likely to be located in a more hydrated region of the interface probably on the waterpool side of the interface.

Fig. 2 also shows that the short lifetime component remained almost constant at around 1 ns within the experimental error over the entire range of ω_0. However, it can be seen that the long fluorescence lifetime component decreased from 3.9 ns ($\omega_0 = 0$) to 2.3 ns by $\omega_0 \approx 5$, and then remained constant at ca. 2.1 ns. The region over which the long fluorescence lifetime component decreased corresponds to the formation of the primary hydration shell in contact with the AOT headgroups, as determined in thermodynamic studies [31]. This implies that the site of NATA is associated with the interfacial region and its microenvironment becomes constant once the surfactant headgroup molecules have been hydrated.

A decrease in the long lifetime component of NATA in reverse micelles over the range of ω_0

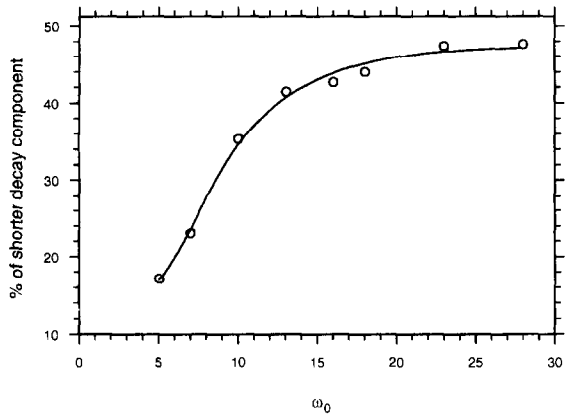

Fig. 3. The percentage of the short component in the fluorescence decay of NATA in reverse micelles with varying ω_0.

values from 0.28–22.4 can also be seen in data presented by Gallay et al. [13], although the authors made no comment on this fact in their discussion. However, this information was not previously observed by Ferreira and Gratton [7] who presented their data globally analysed, thus allowing no variation in the lifetime components. In this work, a global fit of decay curves above $\omega_0 = 5$ gives the fluorescence lifetimes 1.48 ± 0.18 ns and 2.24 ± 0.09 ns with a global χ^2 of 1.59.

From this global analysis, Fig. 3 shows the variation in percentage of the total fluorescence intensity (i.e. relative concentration × fluorescence quantum yield) of the short lifetime component for $5 < \omega_0 < 28$. At higher ω_0 there is no further change. Thus, from Fig. 3 it is evident that, the NATA species producing the short lifetime component becomes increasingly prominent over this medium waterpool size range and by $\omega_0 > 20$ consistency in the environment of the fluorophore has been reached. Thus, assuming that the fluorescence quantum yields of the two NATA species are constant within reverse micelles of varying water content, increasing the waterpool size over the ω_0 range 5–28 favours the population of the NATA excited state with a shorter fluorescence lifetime.

However, consistent with the interfacial location of NATA demonstrated above, it is unlikely that this species of NATA yielding the shorter lifetime component lies completely in the waterpool since it makes up 28% of the decay at $\omega_0 = 0$. However, if there are two distinct sites of NATA, as suggested above, then this result implies that the site of NATA in the non-polar side of the interface becomes more populated as the water content of the reverse micellar solution is increased. This can be explained by considering the polarity of both NATA sites to increase with increasing hydration. This encourages more NATA to move into the less polar of the two sites at high waterpool sizes. Furthermore, it is also interesting to note that at large waterpool sizes the contribution from each component approaches 50%, which is consistent with the NATA molecule existing in two equally populated excited states.

Changes in the steady-state fluorescence intensity and peak wavelength for NATA in reverse micelles with increasing waterpool size were found to be similar to that previously published by Ferreira and Gratton [7]. The spectral peak wavelength increases with increasing waterpool suggesting that the average polarity of the NATA environment increases and/or that the solvent relaxation time increases during the excited state. The decrease in fluorescence intensity with increasing waterpool size also implies an increased average exposure to a more polar environment, as NATA is commonly observed to be quenched by water molecules, probably by proton transfer [32].

According to the time-resolved fluorescence data with respect to NATA existing in two distinct sites, then the indications are that, at high waterpool sizes, more NATA molecules move into the less polar of the two possible locations in the reverse micellar interface. Thus, at high waterpool sizes the average position of NATA is located further away from the waterpool, deeper into the interfacial region. However, the variation in steady-state fluorescence characteristics with waterpool size demonstrates that both possible sites of NATA must become hydrated within reverse micelle solutions of higher water content. Reconciliation of these facts implies that, in general, water increasingly penetrates the reverse micellar interface as the water content of the solution is increased, such that throughout the interface the polarity increases.

Recently it has been suggested that it is physically more meaningful to fit decay data to a distribution of decay times about a mean to allow for the closely spaced energy levels of the different conformations

[33,34]. A top-hat distribution function about a mean lifetime was fitted to the decay data for NATA in AOT reverse micelles. However, the fits were only satisfactory for $\omega_0 > 10$ and there is no obvious physical explanation why the decay would change from a biexponential to a single distribution around this point. The distribution fits show a trend in decreasing mean fluorescence lifetime and width with increasing waterpool size as would be expected to accommodate the two components in the biexponential model. Hence, no further consideration of distributions will be given here.

3.1.1. Multi-wavelength array analysis of NATA

Fig. 4 shows the global wavelength dependence of the longer lifetime component's decay contribution at ω_0 ca. 45. A novel feature of these measurements is that the decay data were acquired at each wavelength simultaneously using an array detection system. This comprises a spectrograph, multi-anode MCP-PM, and multi-channel timing NIM electronics incorporating a single time-to-amplitude converter and an ASIC (application specific integrated circuit)-based routing module for which the principle of operation is described in reference [35]. Simultaneous acquisition using array detection, not only provides a global measurement, but has the advantage of a much reduced overall measurement time, and also eliminates false wavelength trends due to changes in sample condition. The decay data were globally analysed using a biexponential model with

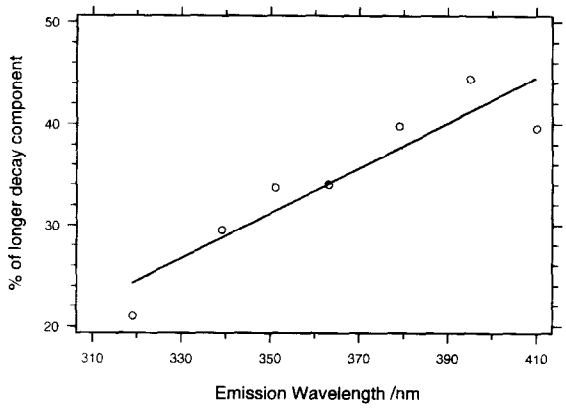

Fig. 4. Multi-wavelength array analysis of NATA in reverse micelles at $\omega_0 = 45$.

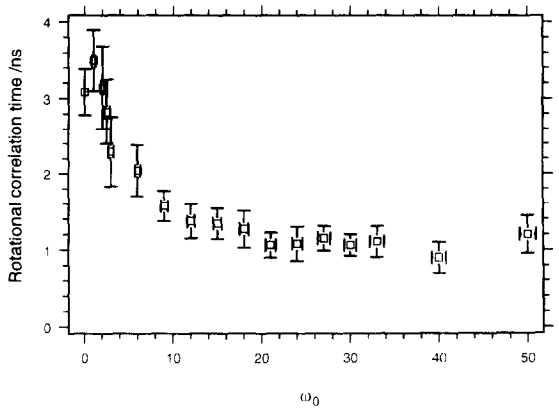

Fig. 5. Variation in rotational correlation time with waterpool size for NATA in reverse micelles.

fixed decay times of 1.33 ns and 2.24 ns. This shows that the long lifetime component corresponds to a spectrally distinct species of NATA at the red edge of the total emission spectrum. This is in agreement with the recent measurements using synchrotron radiation by Gallay et al. [13]. Thus, if it is the case that NATA exists in 2 sites within the reverse micellar structure, then this analysis would suggest the population responsible for the longer component of the fluorescence decay would lie nearest the waterpool. This is completely consistent with the analysis of the lifetime components of NATA in reverse micelles.

3.1.2. Time-resolved anisotropy data

Fig. 5 shows the variation of the characteristic rotational correlation time with increasing waterpool size for NATA in AOT/iso-octane/water reverse micelles, where each data point had an associated χ^2 of between 0.9 and 1.1. As a first approximation, the anisotropy data were fitted with a single mean rotational correlation time. Steady-state anisotropy measurements show a similar shaped profile with increasing waterpool size (not shown here) as previously reported by Ferreira and Gratton [7]. Throughout the measurements, the residual anisotropy (r_∞) was in the range 0.01–0.02 indicating free rotation of the NATA molecule. The initial anisotropy (r_0) decreased slightly, from 0.22 to 0.15 with increasing waterpool size, which may represent an instrumental

effect such as increased scattering, or perhaps the inadequacy of the kinetic model used (i.e. the two NATA species may have different anisotropies).

It can be seen that the initial rotational time for $0 < \omega_0 < 5$ is the highest, implying that the fluorophore is in a more viscous medium. The rotational time is lower with no water present ($\omega_0 = 0$) than with a small amount ($\omega_0 < 2$) which is most likely because at $\omega_0 = 0$ the NATA molecule will be rotating in unison with the micellar structure. However, as the micelle swells, the rotation of the NATA molecule and the micelle become decoupled. This effect has also been seen in the steady-state anisotropy of NATA [7] and recently, for the rotation of a small peptide within AOT reverse micelles [36]. Even by $\omega_0 = 50$ the rotational time is still much greater than that of NATA in aqueous solution (60 ps), indicating that the molecule is associated with the interface to some degree. The constancy in the fluorophore's rotational correlation time for $\omega_0 > 20$ is in agreement with the consistency of the fluorophore's environment at waterpool sizes greater than $\omega_0 = 20$ demonstrated by Fig. 3.

By measuring the steady-state fluorescence intensity and fluorescence depolarisation of auramine O, a probe known to lie at the water/surfactant interface, Hasegawa et al. [37] found the value of η at the interface of AOT reverse micelles to be 120 cP at

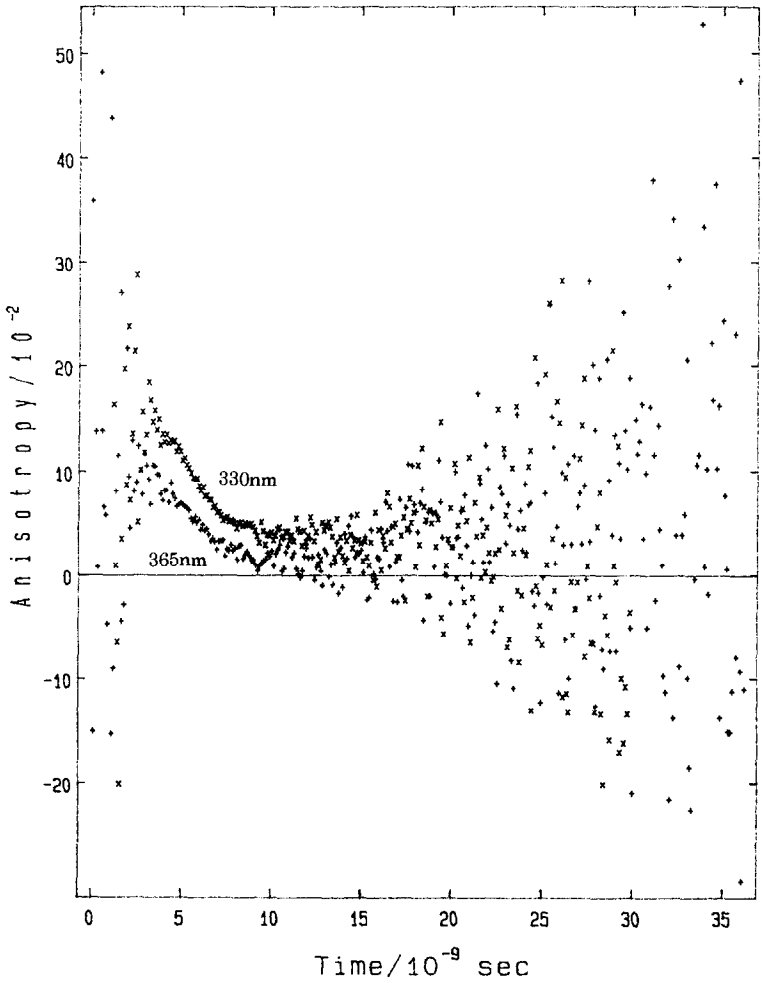

Fig. 6. The time-resolved anisotropy of NATA in AOT reverse micelles ($\omega_0 = 30$) at 330 nm and 365 nm.

$\omega_0 = 2$ which then decreases rapidly reaching a constant value of around 20 cP by $\omega_0 = 20$. Using the Stokes–Einstein relationship (e.g. [25]), and assuming a similar rotating volume of NATA in reverse micelles as in aqueous solution, the rotational correlation times reported here imply that the microviscosity of the environment of NATA is 60 cP at $\omega_0 = 2$ decreasing to 18 cP at $\omega_0 = 20$. The agreement between the trends of these results is further evidence of the interfacial location of NATA.

Fig. 6 shows the wavelength-resolved time-resolved anisotropy of NATA in AOT reverse micelles. These measurements were taken using reverse micellar solutions of composition $\omega_0 = 30$, at which hydration level there is approximately 50% of each excited state decay of NATA in the fluorescence emission (as shown in Fig. 3). The two time-resolved measurements shown were taken using a monochromator to select the emission wavelengths of 330 nm and 365 nm, both with bandwidths of ± 10 nm. For both wavelength selections, the residual anisotropy was found to be practically zero, implying the free rotation of the fluorophore in both cases. However, the rotational correlation times of the blue and red emission differed as 0.72 ± 0.18 ns and 1.65 ± 0.42 ns respectively. This is firm evidence that the two excited states of NATA are located in sites of differing viscosity.

The analysis previously, such as the time-resolved emission spectra and the lifetime data, implies that, if there are two distinct sites of NATA, the red emission from the fluorophore arises from NATA on the waterpool side of the interface, while the blue emission must arise from NATA located on the oil side of the interface. Thus, the information obtained from measuring the wavelength-resolved time-resolved anisotropy of NATA in reverse micelles, implies that the waterpool side of the interface is in fact more viscous than the oil side of the interface. This has not been previously reported, and if correct, should also be evidenced by a difference in the quenching of the fluorescence of the fluorophore in each of the two sites.

3.1.3. Quenching data

Carbon tetrachloride is restricted to the bulk phase and micellar interface (see Fig. 1). Quenching of NATA by CCl_4 in AOT/iso-octane/buffer reverse micelles produces an upward deviation from the Stern–Volmer plot defined in equation (1). There was no change in the Stern–Volmer plot for reverse micelles of varying composition at $\omega_0 = 22$ or 15. At low quencher concentrations (i.e. < 0.25 M), a straight line can be fitted with a weighted average of the individual quenching constants of 7.1 M^{-1} (mean lifetime = 1.6 ns). An equivalent plot for tryptophan in AOT/iso-octane/buffer reverse micelles shows a straight line in the concentration range 0–0.3 M, with a weighted average of the individual quenching constants of 3.9 M^{-1} (mean lifetime = 1.8 ns), implying that NATA is more efficiently quenched by CCl_4 in reverse micelles than is tryptophan.

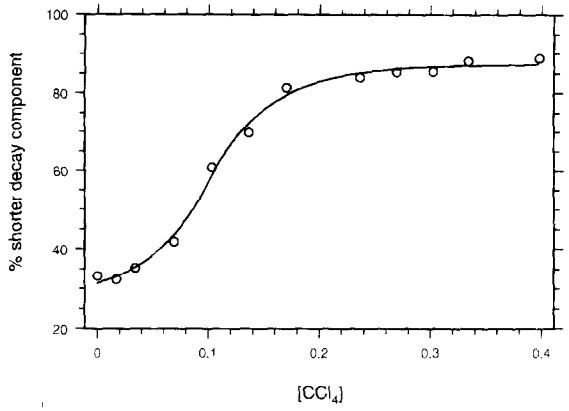

Fig. 7. Variation in the percentage of the short decay component present in the fluorescence of NATA in reverse micelles as carbon tetrachloride is added.

Time-resolved CCl_4 quenching studies of NATA in reverse micelles revealed no change in the measured lifetime of the long component over the range of quencher concentration 0–0.38 M, while the short fluorescence component decreased over this range, such that K_{SV} equals 1.66 M^{-1} for the short component. Also, the relative contribution from the shorter decay component increased from 33% to 88% as subsequent aliquots of quencher were added (see Fig. 7). This implies that the NATA species producing the shorter lifetime component is being dynamically quenched, while the species producing the longer lifetime component is being statically quenched (either by complex formation in the excited state or the proximity of the quencher to the fluorophore being within the quenching sphere of action).

Consideration of the time-resolved anisotropy measurements in Fig. 5, has lead us to conclude that NATA lies in two sites in the reverse micellar system. This idea was first suggested by us, although not proved, in reference [30]. Moreover, Figs. 2 and 4 imply that the site producing the longer fluorescence decay component lies on the waterpool side of the interface, as its lifetime is closer to that of aqueous NATA and appears at the red end of the emission spectrum as shown in Fig. 4. Thus, the results from quenching experiments above would suggest that this population on the waterpool side of the interface is statically quenched by CCl_4 while the population embedded further into the oil phase is quenched by a dynamic process. If this is the case, it requires that carbon tetrachloride is moving slowly through the waterpool side of the interface on the nanosecond timescale. This is consistent with the measurement of the wavelength-resolved rotational correlation time of NATA in the reverse micellar solution reported above. That is, both the quenching data reported here and the measurements of wavelength-resolved time-resolved anisotropy of NATA in AOT reverse micelles reported in Section 3.1.2., coupled with the array analysis reported in Section 3.1.1., provide strong evidence that the waterpool side of the interface is more viscous than the organic side of the interface. All these results and our interpretation of them in terms of the two sites of NATA in AOT reverse micelles are pictorially summarised in Fig. 8.

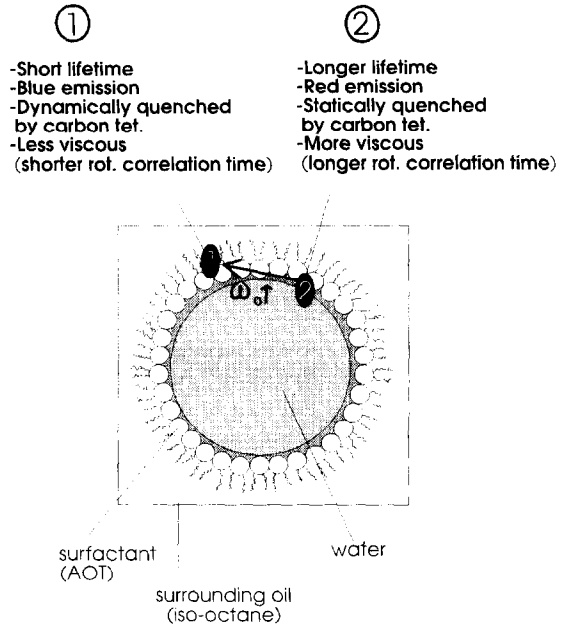

Fig. 8. The two sites of NATA in AOT reverse micelles. Increasing the water content increases the population of NATA in site 1 as indicated by the arrow.

Sodium iodide was used as a hydrophilic quenching agent for NATA in AOT reverse micelles ($\omega_0 = 22$). Using the mean lifetime for the two NATA species, the quenching rate constants for NATA in aqueous solution and AOT reverse micelles are 5.6 M^{-1} ns^{-1} and 0.16 M^{-1} ns^{-1} respectively (using Eqs. (1) and (3)). This implies that the quenching efficiency of NaI on NATA in the waterpool was over an order of magnitude lower than in aqueous solution. This supports the idea that the site of NATA in the reverse micellar system is associated with the interface, with a much more restricted access for the water-based quencher.

3.2. Human serum albumin in reverse micelles

HSA contains a single tryptophan residue and is found to have two distinct fluorescence lifetime components as first noted by de Lauder and Wahl in 1970 [38], although recently some groups report the presence of a third short component when excited at 300 nm [8,39]. In our work, the fluorescence decay of 10^{-5} M HSA in Trizma buffer (pH 7.1) was found to be biexponential with components 3.72 ± 0.45 ns (27.8%) and 7.70 ± 0.09 ns (72.2%), ($\chi^2 = 1.18$). However, as with NATA, HSA in AOT/iso-octane/buffer reverse micelles was found to have a more complicated fluorescence decay. A global analysis of 12 fluorescence decays of HSA in reverse micelles of ω_0 between 9 and 51 gives a very good fit ($\chi^2 = 1.39$) with a triexponential decay of constant decay components 0.87 ± 0.15 ns (17–22%), 3.56 ± 0.18 ns (64–69%), and 9.69 ± 0.54 ns (13–15%). Marzola and Gratton [8] also report a triexponential decay for HSA in reverse micelles with a long lifetime component of 6–7 ns accounting for about 30% of the fluorescence, a component of 2.5 ns (60%) and a 0.5 ns (10%) component.

This suggests that upon incorporation into the reverse micelles the tryptophan residue of HSA is in a different environment from aqueous solution, but that changing the waterpool size has no further ef-

fect. This is reflected in the steady-state anisotropy of HSA in reverse micelles which was found to remain constant at 0.14 over the ω_0 range 10–40. This compares with an aqueous value of 0.04. Furthermore, the emission maxima of the steady-state spectra of HSA in reverse micelles remained at 328 nm in the ω_0 range 10–50 (i.e. blue shifted by 15 nm relative to aqueous HSA). However, this conformation of HSA cannot be the same as thermally denatured aqueous HSA, for which we found the emission maxima to be 338 nm (i.e. blue shifted by 5 nm upon denaturation). This is consistent with ligand binding studies [21,40] which show that upon incorporation in AOT/iso-octane/buffer reverse micelles, HSA undergoes significant change in local and overall conformation.

Time-resolved anisotropy measurements by Marzola and Gratton [8] give a correlation time for the overall protein rotation decreasing from 68 ns at $\omega_0 = 4.1$ to 32 ns at $\omega_0 = 50.4$. The correlation time for the rotation of the fluorophore was also found to decrease, from 1.1 ns to 0.2 ns over the same ω_0 range. Also, studies with the fluorescent probe Nile Red bound to HSA in reverse micelles show changes in the steady-state emission similar to the trends seen for NATA with increasing waterpool size [41]. Thus, in contrast to the numerous measurements cited above, these measurements indicate that increasing waterpool size does have an effect on the local and overall dynamics of HSA. The quenching studies reported below further investigate this change with waterpool size.

3.2.1. Quenching data

Fluorescence quenching of HSA in reverse micelles was studied using both acrylamide and carbon tetrachloride which are soluble in water and oil respectively. Quenching experiments with NATA (Section 3.1.3) showed that CCl_4 can penetrate the micellar interface, and it is possible that acrylamide

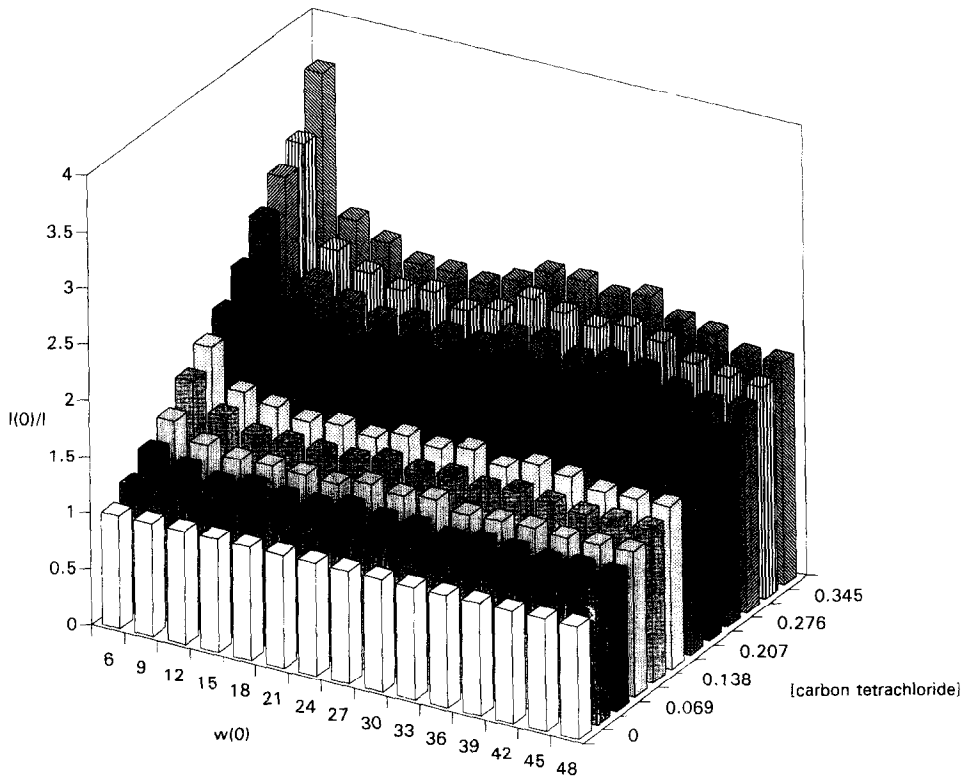

Fig. 9. Steady-state carbon tetrachloride quenching of HSA in reverse micelles at various waterpool sizes. Graph effectively shows the respective Stern–Volmer plots going into the page at various waterpool sizes denoted by the ω_0 value.

can also. The concentrations of acrylamide noted in these experiments refer to that in the waterpool, whereas for carbon tetrachloride the concentration refers to that in the bulk organic phase.

Figs. 9 and 10 show the steady-state Stern–Volmer plots for CCl_4 and acrylamide quenching respectively, of HSA in AOT/iso-octane/buffer reverse micelles measured at fifteen different waterpool sizes from $\omega_0 = 6$ to $\omega_0 = 48$. All plots show an upward deviation from a straight line, but there is a distinct variation in quenching with waterpool size for each quencher. At a very small average waterpool size ($\omega_0 = 6$) it can be seen that (relative to quenching at other waterpool sizes) there is an increase in quenching by carbon tetrachloride and a slight decrease in quenching due to acrylamide. This infers an enhanced exposure of the tryptophanyl residue to the bulk organic solvent at this low waterpool size, which is probably due to a lack of spherical symmetry of the micellar system. In contrast, at large waterpool sizes ($\omega_0 > 30$) the quenching due to acrylamide steadily increases with waterpool size, whereas the quenching due to carbon tetrachloride slightly decreases with waterpool size. This infers that at larger waterpool size the tryptophanyl residue becomes more exposed to the waterpool, which probably occurs as the whole protein moves towards the waterpool from the interface.

In between these two extremes there is a common dip in the variation of quenching with waterpool size for both quenchers centred around $\omega_0 = 21$. This minimum indicates decreased accessibility to the tryptophanyl residue for both quenchers and may imply an interesting conformational change induced in the protein's structure at this waterpool size. This minimum occurs as the waterpool diameter is ca. 80

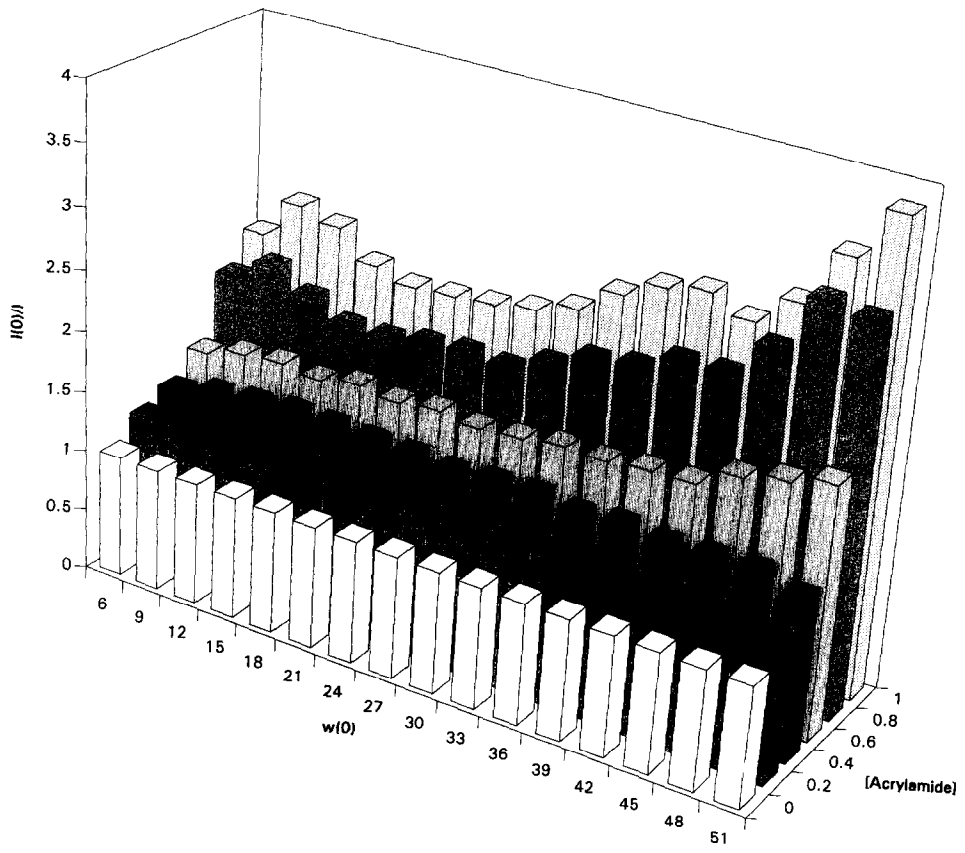

Fig. 10. Steady-state acrylamide quenching of HSA in reverse micelles at various waterpool sizes. Graph effectively shows the respective Stern–Volmer plots going into the page at various waterpool sizes denoted by the ω_0 value.

Å [42] which is about the same size as the HSA molecule, which can be approximated to a solid equilateral triangle of side 80 Å and depth 30 Å [20]. However, it must be noted that this waterpool diameter corresponds with the average value for ω_0, which may or may not be the actual waterpool size for the filled reverse micelles. However, recent light scattering experiments [43] have demonstrated that the incorporation of protein within a reverse micellar solution does not increase the waterpool diameter as significantly as could be expected from the model by Rahaman and Hatton [44].

The Stern–Volmer plots for steady-state quenching by acrylamide of HSA in both aqueous solution and AOT reverse micelles ($\omega_0 = 22$) were found to be both upward sloping. The rate constant found from the initial slope of the curves and the mean lifetime are 0.77 M^{-1} ns^{-1} and 0.022 M^{-1} ns^{-1} for HSA in aqueous and reverse micellar solution, respectively. Again, these values are only a first approximation as the steady-state analysis does not allow the fluorescence decay components to be resolved separately and thus represent a weighted average value for the rate parameter.

Time-resolved quenching of HSA by acrylamide was carried out both in aqueous solution and in AOT/iso-octane/buffer reverse micelles ($\omega_0 = 22$), and the data fitted to a biexponential and triexponential decay model respectively. In the latter case, the shortest fluorescence lifetime component was very fast (i.e. < 0.5 ns), and the other two decay components were fitted to Eq. (2). The results show that dynamic quenching occurs both in aqueous solution (as previously reported and widely discussed [45,46]) and in the reverse micellar solution. The fitted lines produce the Stern–Volmer quenching constants, K_{SV}, and the respective rate constants, k_q, (related by Eq. (3)) as shown in Table 1. The quenching efficiency for acrylamide and the tryptophan residue singlet fluorescence is near unity [47], and so the measured quenching rate constant, k_q, is equal to the diffusion-controlled collisional rate constant. This shows that aqueous HSA is far more accessible to the quencher than HSA in reverse micelles. This is consistent with HSA being associated with the interface, and/or a change in the overall structural conformation upon incorporation into reverse micelles.

Table 1
Stern–Volmer quenching constants and bimolecular rate constants obtained from acrylamide quenching of HSA in aqueous solution and reverse micelles

Sample	Decay component	K_{SV}, M^{-1}	k_q, M^{-1} ns^{-1}
HSA in aqueous solution	1st	2.65 ± 0.04	8.92 ± 1.46
HSA in aqueous solution	2nd	0.71 ± 0.07	5.12 ± 0.86
HSA in reverse micelles	2nd	0.20 ± 0.06	0.49 ± 0.25
HSA in reverse micelles	3rd	0.15 ± 0.04	0.67 ± 0.25

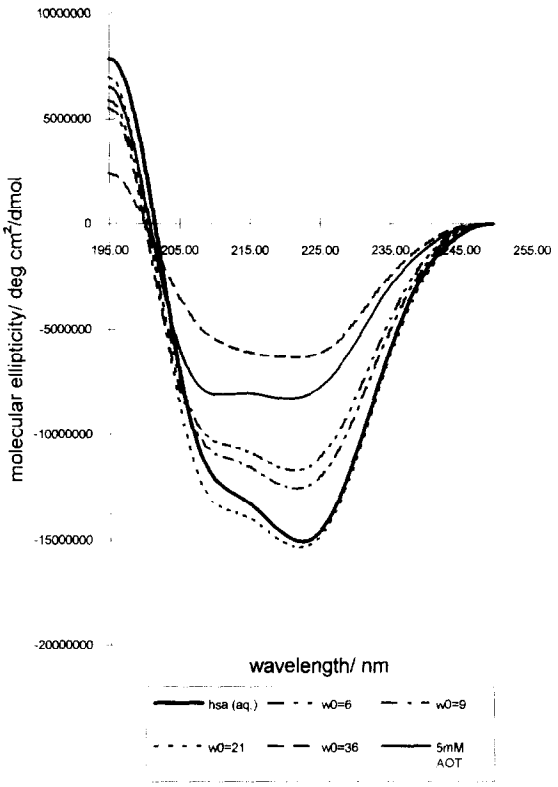

Fig. 11. Far UV CD of HSA in aqueous solution, 5 mM AOT (aq.) and AOT reverse micelles of various compositions.

3.2.2. Circular dichroism

Fig. 11 shows the far circular dichroism (CD) of HSA in AOT reverse micelles of varying waterpool size. The far UV CD spectra shows up the relatively large changes in secondary structure and probably some change in the tertiary structure also [48,49]. It is evident from Fig. 11, that the structure of HSA is similar to its native state in reverse micelles of $\omega_0 = 21$, whereas in reverse micelles of other com-

position there is a marked difference. In particular, there is a loss of helicity in the protein's structure in waterpool sizes other than that corresponding to $\omega_0 = 21$. This loss of helicity may be due to protein-surfactant interactions as the CD spectrum of HSA in 5 mM AOT (aq.) also shows a loss of helicity. However, it should be noted that the subtraction of background circular dichroism due to the reverse micelles of the appropriate composition was performed in each case using unfilled reverse micelles. Thus, if the size of the filled reverse micelles differ from that of the unfilled reverse micelles the background circular dichroism due to the reverse micellar system will be incorrectly compensated for. This effect may be significant, as the average scattering intensity of reverse micelles is highly dependent on the water content [50].

It is interesting that work by Imre and Luisi [51] shows that for long chain nucleic acids (> 20 kDa) there is an increase in the chain rigidity upon incorporation into reverse micelles. It was suggested that the lower dielectric constant in the micellar system causes increased hydrogen bonding within the chain and hence an increased helical content. If it is the case that reverse micelles can be used to control the proportion of helical structure within the protein, it may be a very useful tool for studying the fundamental process of protein folding. It also interesting to note that the molecular chaperone, GroEL, has a central cavity of width about 70 Å (which expands slightly on binding to GroES) in which nascent protein chains probably fold 'in vivo' [6,52]. Thus, it may be that this compartmentalisation induces a conformational change in the protein folding intermediate, in the same way that occurs in reverse micelles of ω_0 ca. 21 as shown here.

A loss of helicity was also seen in bovine serum albumin (BSA) upon incorporation into AOT reverse micelles (although no change was found in reverse micelles of varying composition) [53], and a similar loss of helicity was found for BSA adsorbed on finely dispersed silica particles [54], which suggests a general phenomena of structural change for proteins at interfaces, probably caused by electrostatic interactions. It is probable these electrostatic interactions induce the formation of helical structures in some proteins with low helicities and the disruption of some helical structures in proteins with high helicities, as seems to be the case for proteins in reverse micelles [53].

It is yet to be seen what general principles are followed for all proteins in reverse micelles, and/or for all types of protein compartmentalisation. In particular, it is important to determine whether the photophysical observations reported here are common trends seen for proteins in reverse micelles or atypical processes occurring for HSA within AOT reverse micelles. Similar studies using other protein/surfactant systems are thus required, and are currently being carried out in our laboratories.

4. Conclusions

The behaviour of HSA in reverse micelles is a particular case where the tryptophan residue is found in a hydrophobic pocket of the native protein structure whereas NATA in reverse micelles models the photophysics of an exposed tryptophan. This study shows that for NATA the two distinct excited states in reverse micelles are due to two locations of the probe within the interfacial region. The schematic diagram in Fig. 8 summarises our interpretation of the fluorescence data for NATA in terms of these two sites.

HSA is also associated with the interfacial region, and there is a minimum of quenching by both CCl_4 and acrylamide observed around $\omega_0 = 21$. This is due to changes in the protein's conformation with waterpool size, as seen through changes in the protein's circular dichroism. The protein is most like its native conformation at $\omega_0 = 21$ at which the waterpool size approximates to the same size as the protein molecule. If this is not a result particular to HSA, this may be correlated with the peak enzyme activity often observed in reverse micelles of a particular waterpool size and may be relevant to other instances where proteins are compartmentalised such as in the GroEL-GroES complex during protein folding in vivo.

Acknowledgements

DMD and DM acknowledge financial support from the EPSRC and ICI/Zeneca under the Co-operative Awards Scheme.

References

[1] P.L. Luisi, M. Giomini, M.P. Pileni and B.H. Robinson, Biochim. Biophys. Acta, 947 (1988) 209.
[2] G.A. Krei and H. Hustedt, Chem. Eng. Sci., 47(1) (1992) 99.
[3] A.J. Hagan, T.A. Hatton and D.I.C. Wang, Biotechnol. Bioeng., 35 (1990) 955.
[4] A.J Hagan, T.A. Hatton and D.I.C. Wang, Biotechnol. Bioeng., 35 (1990) 966.
[5] R. Hlodan and F.U. Hartl, in R.H. Pain (Editor), Mechanisms of Protein Folding, Oxford University Press, Oxford, 1994, p. 194.
[6] F.U. Hartl, Nature, 371 (1994) 557.
[7] S. Ferreira and E. Gratton, J. Mol. Liquids, 45 (1990) 253.
[8] P. Marzola and E. Gratton, J. Phys. Chem., 95 (1991) 9488.
[9] N. Unwin and R. Henderson, Scientific American, 84 (1986) 56.
[10] Y.L. Khmelnitsky, A.V. Kabanov, N.L. Klyachko, A.V. Levashov and K. Martinek, in M.P. Pileni (Editor), Structure and Reactivity in Reverse Micelles, Elsevier, Amsterdam, 1989, p. 230.
[11] M.R. Eftink, Biophys. J., 66 (1994) 482.
[12] E.A. Lissi, M.V. Encinas, S.G. Bertolotti, J.J. Cosa and C.M. Previtali, Photochem. Photobiol., 51(1) (1990) 53.
[13] J. Gallay, N. Veshkin, J. Sopkova and M. Vincent, SPIE Proc., 2137 (1994) 390.
[14] K. Bhattacharyya and S. Basak, Biophys. Chem., 47 (1993) 21.
[15] J. Gallay, M. Vincent, C. Nicot and M. Waks, Biochemistry, 26 (1987) 5738.
[16] M. Gonnelli and G.B. Strambini, J. Phys. Chem., 92 (1988) 2854.
[17] C. Nicot, M. Vacher, M. Vincent, J. Gallay, M. Waks, Biochemistry, 24 (1985) 7024.
[18] G.B. Strambini and M. Gonnelli, J. Phys. Chem., 92 (1988) 2850.
[19] A.J.W.G. Visser, J. van Engelen, N.V. Visser, A. van Hoek, R. Hilhorst and R.B. Freedman, Biochim. Biophys. Acta, 1204 (1994) 225.
[20] X.M. He and D.C. Carter, Nature, 358 (1992) 209.
[21] B. Desfosses, N. Cittanova, W. Urbach and M. Waks, Eur. J. Biochem., 199 (1991) 79.
[22] M.P. Pileni, Structure and Reactivity in Reverse Micelles, Elsevier, Amsterdam, 1989, p. 44.
[23] C. Petit, P. Brochette and M.P. Pileni, J. Phys. Chem., 90(24) (1986) 6517.
[24] D.J.S. Birch and R.E. Imhof, Rev. Sci. Instrum., 52 (1981) 9.
[25] J.R. Lakowicz, Principles of Fluorescence Spectroscopy, Plenum Press, New York, 1983.
[26] M. Van der Auweraer and F.C. de Schryver, in M.P. Pileni (Editor), Structure and Reactivity in Reverse Micelles, Elsevier, Amsterdam, 1989, p. 70.
[27] M.H. Gehlen and F.C. de Schryver, Chem. Rev., 93 (1993) 199.
[28] A. Grinvald and I.Z. Steinberg, Biochim. Biophys. Acta, 427 (1976) 663.
[29] J.M. Beechem and L.M. Brand, Ann. Rev. Biochem., 54 (1985) 43.
[30] D.M. Davis, D. McLoskey, D.J.S. Birch, R.M. Swart, P.R. Gellert and R.S. Kittlety, SPIE Proc., 2137 (1994) 331.
[31] P.L. Luisi, G. Haring, M. Maestro and G. Rialdi, Thermochim. Acta, 162 (1990) 1.
[32] H.-T. Yu, J. Colucci, M.L. McLaughlin and M.D. Barkley, J. Am. Chem. Soc., 114 (1992) 8449.
[33] E. Gratton, N. Silva, G. Mei, N. Rosato, I. Salvini and A. Finazzi-Agro, Int. J. Quant. Chem., 42 (1992) 1479.
[34] J.R. Alcala, E. Gratton and F.G. Prendergast, Biophys. J., 51 (1987) 925.
[35] D.J.S. Birch, D. McLoskey, A. Sanderson, K. Suhling and A.S. Holmes, J. Fluorescence, 4(1) (1994) 91.
[36] G. Hungerford, F. Donald, B.D. Moore and D.J.S. Birch, SPIE Proc., 2137 (1994) 554.
[37] M. Hasegawa, T. Sugimura and K. Kuraishi, Chem. Lett., 7 (1992) 1373.
[38] W.B. de Lauder and P. Wahl, Biochem. Biophys. Res. Commun., 42(3) (1970) 398.
[39] K. Vos, A. van Hoek and A.J.W.G. Visser, Eur. J. Biochem., 165 (1987) 55.
[40] B. Desfosses, C. Nicot and M. Waks, Biochem. Int., 26(2) (1992) 257.
[41] D.M. Davis and D.J.S. Birch, J. Fluorescence (in press).
[42] K. Kalyanasundaram, Photochemistry in Microheterogeneous Systems, Academic Press, London, 1987.
[43] S. Christ and P. Schurtenberger, J. Phys. Chem., 98 (1994) 12708.
[44] R.S. Rahaman and T.A. Hatton, J. Phys. Chem., 95 (1991) 1799.
[45] M.R. Eftink and C.A. Ghiron, Biochim. Biophys. Acta, 916 (1987) 343.
[46] M. Punyiczki, J.A. Norman and A. Rosenberg, Biophys. Chem., 47 (1993) 9.
[47] M.R. Eftink and C.A. Ghiron, Biochemistry, 15(3) (1976) 672.
[48] W.C. Johnson Jr., Proteins: Struct. Func. Genet., 7 (1990) 205.
[49] P. Manavalan and W.C. Johnson Jr., Nature, 305 (1983) 831.
[50] J. Ricka, M. Borkovec and U. Hofmeiser, J. Phys. Chem., 94(12) (1991) 8503.
[51] E.V. Imre and P.L. Luisi, Bioch. Biophys. Res. Commun., 107(2) (1982) 538.
[52] K. Braig, Z. Otwinoski, R. Hedge, D.C. Boisvert, A. Joachimiak, A.L. Horwich and P.B. Sigler, Nature, 371 (1994) 578.
[53] K. Takeda, K. Harada, K. Yamaguchi and Y. Moriyama, J. Coll. Int. Sci., 164 (1994) 382.
[54] W. Norde and J.P. Favier, Colloid Surf., 64 (1992) 87.